The Influence of Land Use and Land Cover Change on Landslide Susceptibility in the Lower Mekong River Basin

Chelsea Dandridge[1], Thomas Stanley[2,3,4], Dalia Kirschbaum[2], Pukar Amatya[2,3,4], Venkataraman Lakshmi[1]

1. Engineering Systems and Environment, University of Virginia, Charlottesville, VA 22904, USA
   Corresponding author e-mail address: cld9mt@virginia.edu
2. Hydrological Sciences Laboratory, NASA Goddard Space Flight Center, Greenbelt, MD 20771, USA
3. University of Maryland, Baltimore County, Baltimore, MD 21250, USA
4. Goddard Earth Sciences Technology and Research II, Baltimore, MD 21250, USA

Abstract

The Lower Mekong River Basin in Southeast Asia experiences frequent rainfall-triggered landslides especially during the monsoon season. In this study, the influence of land use and land cover (LULC) change and other causative factors on landslide susceptibility is evaluated in the Lower Mekong Basin. Frequency ratio analysis is performed to quantify the relationship between LULC change and susceptibility. Detailed landslide inventory maps are used for analysis with yearly LULC maps. The LULC change is used as a contributing variable in a logistic regression-based susceptibility model with other variables including distance to roads, slope, aspect, forest loss, and soil properties. The Receiver Operating Characteristic (ROC) curve and Area Under the Curve (AUC) are estimated for the model trained by each landslide inventory. The models show good performance, with AUC values ranging from 0.697 to 0.958 and an average AUC equal to 0.820. Both the Frequency Ratio analysis and the Logistic Regression models indicate LULC change from agricultural land to forest has a positive correlation with landslide occurrence. The most significant factors in the models are found to be distance to roads, slope, and aspect. A better understanding of the effects of LULC on landslide susceptibility can be useful for local land and disaster management and for the implementation of LULC as a factor in future susceptibility models. Using datasets that are unique to the Lower Mekong region, this study provides additional insights into the relationship between causative factors and landslide activity to better inform regional and global landslide susceptibility modeling.

Keywords: land use; land cover change; Lower Mekong River Basin; landslides; logistic regression; susceptibility mapping

1.0 Introduction

A landslide encompasses a wide range of mass movements and can be defined as the downslope movement of soil, rock, or earth (Highland & Bobrowsky, 2008). The movements can be triggered by various external activities such as intense rainfall, earthquakes, changes in water level, waves, or stream erosion, which lead to a decrease in shear strength and an increase in shear stress on the slope (Dai et al. 2002). Landslides can also be caused by anthropogenic activities such as excavation, road construction, and land use changes. These factors often induce small, shallow landslides, but abrupt changes to the slope surface such as poor construction and planning can result in larger, more dangerous landslides (Jaboyedoff et al. 2016). Watersheds that have been recently affected by wildfires can be highly susceptible to rainfall-triggered landslides that usually occur within a short time following the burn (Degraff et al. 2015; Kean et al. 2011). This study focuses on rainfall-triggered landslides as they are the most frequent and cause loss of life and destruction of property across the globe (Froude & Petley 2018). Rapid urbanization can increase the risk for landslides, especially along poorly constructed roads and deforested areas in mountainous regions (Forbes et al. 2012). However, better land management of forests and cultivated areas can produce a decrease in rainfall-triggered landslide susceptibility (Pisano et al. 2017).

In the Lower Mekong River Basin (LMRB) in Southeast Asia, the monsoon season brings an increase in flood and landslide disasters due to an increase in rainfall from large storms in combination with the complex topography of the region. The LMRB has experienced extensive changes from urban and agricultural expansion, deforestation, river damming, and natural disasters such as flood and drought. In this region, changes in Land Use and Land Cover (LULC) are largely influenced by agricultural prices, road accessibility, construction projects, and climate change (Spruce et al. 2020). Spruce et al. (2020) assessed LULC changes in the Lower Mekong using two maps from 1997 to 2010. In their analysis, 2.5% of the total area of permanent agriculture decreased which could be associated with the abandonment of crops or converting cropland to forests. They also identified an 6.7% increase of the total area categorized by scrub/shrub/herbaceous which could be attributed to abandoned cropland reverting back to forest. Looking at the changes between LULC classes, some cropland had changed to deciduous forest/scrub over time between 1997 and 2010. Changes in land cover can have variable impacts on landslide susceptibility. In some cases, human impacts such as deforestation and mining serve to exacerbate instability on slopes (Winter et al. 2010). In other examples, thoughtful engineering and planning can serve to stabilize slopes (Prastica et al. 2019; Yan et al. 2019).

The preconditions for landslides vary, but changes in land use and land cover (LULC) have been shown to have local impacts (e.g., Glade 2003; Hewawasam 2010; Mugagga et al. 2012; Reichenbach et al. 2014). Pisano et al. (2017) evaluated how land cover change affects slope stability over time in the Italian Southern Apennine Mountains by treating land cover as a dynamic variable, unlike many other landslides susceptibility studies that consider land cover as a static variable. This study found that a decrease in forest and cultivated land and increase in barren, pasture, and shrub land led to an increase in landslide susceptibility. A study by Persichillo et al. (2017) assessed shallow landslides in the northern Apennine Mountains in Italy in areas with land abandonment and changes in land management practices from 1954 to 2012. They found that cultivated lands that were abandoned and allowed to gradually recover naturally was the land cover change scenario most susceptible to landslides and

land cover was the most predisposing factor in all study areas. Similarly, Deng et al. (2018) investigated landslide distribution and agricultural abandonment in several provinces in China's mountainous areas. They concluded that more landslides occurred in areas with high incidence of agricultural abandonment. Furthermore, the effects of land use changes on landslides were analyzed in a landslide-prone region in Northeast Turkey with mountainous topography and high rainfall frequency by Karsli et al. (2009). Land cover changes and landslides were identified using aerial images taken in 1973 and 2002. Their results indicated that the land cover type played an important role in landslide occurrence as 95% of the landslides identified from the imagery were in areas with acidic soil weakened by fertilizer use in agriculture.

Frequency Ratio (FR) analysis is a common method used to assess the relationship between susceptibility and the occurrence of a landslide event (Gariano et al. 2018; Pourghasemi et al. 2013). A study by Silalahi et al. (2019) used GIS mapping and FR analysis to assess the effects of contributing factors on landslides in Bogor, Indonesia. Their results indicated land cover as one of the most important factors contributing to landslides as well as lithology and soil type in this area. Additionally, Khan et al. (2019) used the FR to create a landslide susceptibility index which was used to produce a susceptibility map for northern Pakistan. Their study found barren land and irrigated agricultural land to have the highest FR values of the land cover classifications, however distance to roads was found to have the highest overall FR value. These and other studies use FR to assess conditioning factors and create susceptibility maps but however, rarely incorporate land cover as a dynamic variable. Additionally, statistical methods like Logistic Regression (LR) are effective in identifying input variable importance/significance and several studies have considered LULC within this framework (e.g., Reichenbach et al. 2018; Lee & Sambath 2006; Shahabi et al. 2014; Bai et al. 2010; Das & Lepcha 2019; Bornaetxea et al. 2018). LR has been an effective tool for developing landslide susceptibility maps and highlighting the significance of contributing variables however, few studies have considered how LULC can be considered dynamically in these models to explain changes over time in a region. Hemasinghe et al. (2018) analyzed susceptibility in mountainous regions predisposed to landslides in Sri Lanka. Their study examined slope, aspect, lithology, land cover, distance to rivers and roads as predictor variables. Land cover was determined to be the most influential factor in the study area. Known landslide locations were used to validate their susceptibility map, and a majority (76%) of the landslide points were in high and extremely high susceptibility areas. Land cover is similarly used as a static predictor variable in many other susceptibility studies, uniquely this study will treat land cover change as a dynamic variable that changes over time.

The question posed in this study is - how do changes in land use and land cover (LULC) impact landslide susceptibility in the LMRB? We evaluate these interactions using several new landslide event inventories mapped between 2015 – 2018 that provide information within areas of Vietnam, Myanmar, and Laos (Amatya et al. 2021)(Figure 1). Additionally, this study closely examines the effects of LULC change on landslide occurrence, a dynamic which is not completely understood in the LMRB (Shu et al. 2019). Our work seeks to understand the relationship of changing LULC over time and how this impacts susceptibility. The relationship between LULC changes and landslide occurrence will be analyzed using Frequency Ratio (FR) analysis and Logistic Regression (LR) modeling. The FR will be used to closely examine the frequency of landslides within the various LULC

change scenarios present in each of the landslide inventory locations. This study will use the LR models to compare LULC changes with other contributing factors like slope, forest loss, soil properties described in Table 2. The FR and LR results will be compared to determine any similarities regarding the significance of LULC changes on landslide occurrence. Results of this work are important as population expansion, road development and farming continue to increase (and hence changes in land cover) in the LMRB (Spruce et al. 2018). This work is part of a broader effort to characterize landslide susceptibility, hazard, and exposure within the LMRB for decision making at the country and municipal level using satellite remote sensing products.

2.0 Data

2.1 Landslide Inventory

The landslide inventories used in this research were mapped utilizing high-resolution satellite imagery from Planet (Planet Team, 2017) using the modified framework of Semi-Automatic Landslide Detection (SALaD) system (Amatya et al. 2021a). SALaD uses object-based image analysis and machine learning to map landslides. As we are focusing on rainfall event-based inventories, it is important we map landslides induced by that event only as pre-event landslides may have been triggered by phenomena such as earthquakes. A change detection-based approach was introduced to the SALaD framework (SALaD-CD) utilizing pre- and post-event imagery (Amatya et al. 2021b). The new framework incorporates image normalization, image co-registration and change detection. The landslide polygons produced by SALaD-CD were manually corrected and converted to initiation points using NASADEM (NASA JPL 2020). A total of 18 rainfall-triggered landslide inventories between 2015 and 2018 were used in this analysis: 13 in Vietnam, three in Myanmar, and two in Laos (Figure 1). Details on the landslide inventories used in this study are provided in Table 1.

2.2 Digital Elevation Model (DEM)

NASADEM with 30 m spatial resolution was used to derive the input variables for slope and aspect (NASA JPL 2020). NASA DEM is derived from SRTM, which was launched in 2000, with processing improvements, elevation control, void-filling and merging with data that was unavailable at the time of the mission. NASADEM also provides an improved spatial resolution from the original three-arcsecond SRTM DEM to one-arcsecond, making it the finest resolution, global, freely-available DEM product. Slope is one of the major influencers of landslide activity, and therefore was selected based on its likely correlation with landslide susceptibility (Bruschi et al. 2013; Chen et al. 2019; Indhanu et al. 2020). The aspect is derived using GIS and reclassified to represent North, South, East, and West facing slopes. Data is publicly available from https://doi.org/10.5067/MEaSUREs/NASADEM/NASADEM_HGT.001.

2.3 Land Use/ Land Cover (LULC)

Land use and land cover (LULC) data from the Regional Land Cover Monitoring System (RLCMS) is available via the SERVIR-Mekong Land Use Portal and is presented at 30 m spatial resolution and yearly temporal resolution from 1987 to 2018 for the Lower Mekong River Basin (Saah et al. 2020). The RLCMS uses

historical Landsat and MODIS data to create LULC maps. The methodology behind deriving the maps can be summarized, defining the classification typologies, creating the primitive layers using supervised classification and machine learning algorithms, combining the primitive layers into land cover maps, and lastly, an accuracy assessment. The typology classifications were determined by stakeholders from Cambodia, Laos PDR, Myanmar, Thailand, and Vietnam. LULC data from ten years prior to each landslide event, spanning from 2005 to 2018, were used for analysis in this study. Due to limited spatial representation of the original classifications, the land cover was reclassified into three categories shown in Table 3, similarly to the methodology in Chen et al. (2019). For more information on how this dataset was created and its details, please review Saah et al. (2020). Data is publicly available from https://landcovermapping.org.

2.4 Roads

Proximity to roads has been found influential on rainfall-triggered landslide occurrence in several areas in previous studies (Larsen & Parks 1997; Penna et al. 2014; McAdoo et al. 2018). The construction of roads changes the hydrologic response and surface and subsurface flow paths in the affected area which can influence landslide susceptibility (Penna et al. 2014). McAdoo et al. (2018) found that within 100m of a road rainfall-triggered landslides were more than two times as likely to occur in Nepal. The Global Roads Inventory Project (GRIP) is compiled from publicly available national vector datasets from governments, research institutes, NGOs and crowd-sourcing initiatives and includes over 21 million km of roads. The GRIP dataset is available as a vector dataset for each region of the world. The Southeast Asia GRIP dataset was used to derive a distance to roads raster which represents the distance to nearby roads for each pixel in the selected extent using GIS software for each landslide inventory location. For more information on how this dataset was created and its details, please refer to Meijer et al. (2018). Data is publicly available from https://www.globio.info/download-grip-dataset.

2.5 Soil Properties

The World Soil Information Service (WoSIS) provides standardized soil profile data for various environmental applications at global scale. The most current WoSIS snapshot is a compilation of nearly 200,000 soil profiles from locations across the globe. These profiles are standardized and distributed using a database model, SoilGrids, which uses machine learning methods to map the spatial distribution of soil properties based on the soil profile observations (Hengl et al. 2017). Soil data is available for six standard depth intervals at 250 m spatial resolution. For a full description of this data, please refer to Batjes et al. (2020). Two soil layers representing bulk density and organic carbon were downloaded from SoilGrids for each study region at the at 0 – 5 cm depth. These variables were resampled to the resolution of the DEM at 30 m for model implementation. Data is publicly available from www.soilgrids.org.

2.6 Forest Cover Loss

Global Forest Change data is created from Landsat imagery at 30 m spatial resolution and characterizes forest extent, loss, and gain and is available from 2000 to 2019. In this study, this data is used to estimate the Forest Loss over the past ten years for each landslide inventory extent. For more information on the methodology

and details of this dataset, please review Hansen et al. (2013). Data is publicly available from http://earthenginepartners.appspot.com/science-2013-global-forest.

3.0 Methodology

3.1 LULC Analysis

The landcover maps were reclassified from nine categories to three broader categories due to the limited spatial representation of the original land cover classifications in the small extents represented by the landslide inventory locations. These reclassification categories as well as the original categories represented in the study area described in Table 3 and shown in Figure 2 for the greater Lower Mekong region. The reclassified landcover maps were analyzed to estimate the amount and type of change over the 10-year time period prior to the landslide event in each study region as well as the overall LULC patterns in the greater Lower Mekong region from 1998 to 2018. Overall, the time frame used to analyze LULC changes varies in the literature. Several studies chose time intervals that ranged from five to 30 years due to the availability of aerial imagery (Karsli et al. 2009; Persichillo et al. 2017). The 10-year time period was selected based on previous studies that assessed LULC changes over time (Chen & Huang 2013). Chen and Huang (2013) compared LULC changes over 10 years (1999 to 2009) to determine the relationship between LULC change and landslides triggered by Typhoon Morakot in Taiwan. They found that areas with a change in land cover had a higher frequency of landslides than non-changed areas. Here, the LULC change over the ten-year time-period was estimated by assigning a change scenario to each pixel based on its land cover classification in the two maps (i.e., map of landcover in 2018 compared to the map of landcover in 2008). There is a total of nine possible LULC scenarios for each pixel including three no-change scenarios where the type of land cover classification did not change over the specified time-period. The percentage of total area of each LULC scenario is estimated and reported for each landslide inventory location and shown in Figure 3 (A) and averaged over all locations in Figure 3 (B). Land cover classified as urban represents less than 1% in each study area except for one inventory, Nha Trang (NH), which is composed of 16% urban area. Only three of the inventories are characterized by greater than 25% agricultural area (Figure 3A). Forests comprise over 50% of each area and 81% of the total area used for analysis. The LULC change scenario with the largest area represented in the study locations is from agriculture to forest, representing 2% of the total area and less than 5% in each inventory extent (Figure 3B).

3.2 Frequency Ratio Analysis

Frequency ratio (FR) was used in this study to quantitatively examine the relationship between landslide occurrence and each LULC change scenario. The FR is the ratio of the percentage of landslide occurrence in a factor class to the total percentage of that factor in the area, and the average FR value is one (Khan et al. 2019). Values greater than one indicate that landslides occur more frequently relative to the total distribution within the variable being considered over the study area. FR values lower than one indicate a lower amount of landslide occurrence (Gariano et al. 2018). The equation used to calculate FR is as follows:

$$FR = \frac{M_i / \sum M_i}{N_i / \sum N_i} \qquad (1)$$

Where M_i = number of pixels containing landslides in LULC class i, $\sum M_i$ = total number of pixels containing landslides in the study area, N_i = total number of pixels in the study area for that particular LULC class, and $\sum N_i$ = total number of pixels in the study area. The FR of each LULC scenario is estimated for each study location.

3.3 Logistic Regression

A logistic regression model is used in this study to further assess the relationship between changes in LULC and landslide occurrence as well as determine any similarities with the results of the Frequency Ratio analysis. The model is outlined in the workflow diagram shown in Figure 4. Many susceptibility studies use logistic regression to evaluate binary response variables such as landslide occurrence (Lombardo & Mai 2018; Horafas & Gkeki 2017; Pourghasemi et al. 2013). Logistic regression models the probability of events based on the linear combination of independent contributing variables (Camilo et al. 2017). The model produces coefficients for each input variable, which are used to predict the probability of landslides over the study area. Positive coefficients indicate that there is positive correlation with the presence of this conditioning factor and landslide occurrence, and negative coefficients indicate a negative correlation between presence of the factor and landslide occurrence and there is an absence of this factor in locations where landslides occur. The predictions are used with raster data of each contributing variable to create a landslide susceptibility map. The equations used in logistic regression are as follows:

$$P = \frac{1}{1 + e^{-Z}} \qquad (2)$$

$$Z = b_0 + b_1 x_1 + b_2 x_2 + \cdots + b_n x_n \qquad (3)$$

Where P = probability of occurrence of the event occurring, Z = linear combination, b_0 = intercept, b_i = slope coefficients, and x_i = independent variables (Lee & Sambath 2006). To create training and testing datasets, an equal number of non-landslide points are generated. The logistic regression model is used to create landslide susceptibility maps for each of the 18 study regions mapped in the landslide event inventory. The model is trained with 70% of the landslide inventory as well as randomly generated points that do not coincide with landslide locations. The following predictor variables are tested in the logistic regression model in this study: slope, aspect, LULC change, distance to roads, bulk density, organic carbon, and forest loss. These variables were selected based on their spatial and temporal availability and potential correlation with landslide occurrence as well as their significance in the logistic regression models determined by their corresponding p-values. A significance level of 0.01 implies there is less than 0.1 % chance that the coefficient may be equal to zero and therefore be insignificant in determining landslide susceptibility. A p-value less than 0.05 is statistically significant and p-values greater than 0.05 are determined as not statistically significant. All of the model input variables were reclassified into

categorical factors for simplified comparison between the categories. The classifications of each factor are shown in Table 4. These maps were validated using the Receiver Operating Characteristic (ROC) curve and Area Under the ROC Curve (AUC) analyses, common statistics for assessing the predictive capacity of susceptibility models (Felicísimo et al. 2013). The ROC was derived using a testing dataset that is comprised of 30% of the landslide inventory as well as randomly generated non-landslide points. These metrics are often considered to evaluate the performance of susceptibility models and the model with a larger AUC value is considered better predictive model (Gorsevski et al. 2006; Zhou et al. 2018; Lombardo & Mai 2018).

4.0 Results

Eighteen landslide inventories were used in this study to assess the relationship between land cover change and landslide occurrence. The percentage of total area represented by each LULC scenario averaged over all inventory locations is shown in Table 5. The number of total landslides occurring in each LULC scenario from the 18 inventories are shown in Table 6. The Frequency Ratio value averaged over all inventories for each LULC scenario is shown in Table 7. The category forest with no change in LULC over ten years prior to the landslide event made up about 82% of the total area when averaging over all 18 inventory locations (Table 5). The majority of landslides (15,568) also occurred within this LULC category (Table 6). The average FR for Forest with no change was 2.06 (Table 7). The category making up the second largest percentage of total area is agricultural land with no change over ten years prior to the landslide event, which composed about 15% of the total area (Table 5). This LULC category experienced 2,530 landslides (Table 6) and had an average FR of 1.64 when averaged over all locations (Table 7). The category of urban with no change represented about 1% of the total area within the 18 inventory locations (Table 5) and experienced no landslides. The LULC change scenario from agriculture to forest in the ten years prior to the landslide event comprised only 2.1% of the total area within all inventory locations (Table 5). However, this area experienced 614 landslides (Table 6) and had an average FR of 2.83 (Table 7) for all locations. The results of the FR analysis could indicate that areas experiencing a change from agriculture to forest are more susceptible to landslides than other land cover change scenarios.

The Frequency Ratio (FR) aids in understanding location specific conditions for landslide occurrence by providing the ratio of the landslide area to the total area. Figure 5 shows a matrix diagram of the FR for each landslide inventory and LULC change scenario. FR values less than one are represented by dark blue. From Figure 5, we can see that all categories including urban produced FR values less than one. The scenario from forest to agriculture was only found significant in the Sin Ho, Vietnam with a FR of 1.63 and Hakha, Myanmar with a FR of 1.94. The scenario agriculture with no change in ten years prior to the landslide event had FR values greater than one for half of the inventory locations. Forests with no change had FR values greater than one for all but one location (Tam Duong, Vietnam). However, the highest FR values were for the LULC change scenario from agriculture to forest, ranging from 0 to 8.15 over the 18 landslide inventory locations. This scenario had relatively high FR values of 5.14 for Nha Trang, Vietnam; 6.33 for Vi Xuyen, Vietnam; 6.72 for Muong La, Vietnam; and the highest FR value of 8.15 for the landslide inventory in Phu Yen, Vietnam. The change observed from

agriculture to forest could be a representation of agricultural abandonment, where the agricultural fields are left to naturally recover and revegetate. Spruce et al. (2020) observed similar changes from agriculture to forest in the Lower Mekong between the period from 1997 to 2010. These high FR values could be explained by agricultural abandonment practices having an impact on landslide occurrence which would be consistent with the results found by Deng et al. (2018) and Persichillo et al. (2017).

In addition to assessing the LULC within the extents of the 18 landslide event inventories, land cover changes were also analyzed over the greater Lower Mekong region from 1998 to 2018. Figure 6 shows the area in square km represented by each LULC category over the entire Lower Mekong region and a noticeable change in land use between 1998 and 2001. The urban areas increased by 11.3% from 1998 to 2001 and increased constantly at an average rate of 1.2% per year. The area represented by forests decreased by 5.5% of the total area from 1998 to 2001 with an average decrease of 0.3% per year. In contrast, the amount of agricultural area increased drastically by 11.6% from 1998 to 2001 with an average increase of 0.6% per year. The percentage of total area represented by each of the three LULC categories from 1998 to 2018 are shown in Figure 7. From this figure we can observe that the amount of agricultural land increased by approximately the same area that of which the forests decreased from 1998 to 2001. Figure 7 shows that the majority of the Lower Mekong region is forested ranging from 67 – 63% of the total area for the time period from 1998 to 2018. About a third of the area is classified as agricultural land, ranging from 30 – 34%, and the smallest percentage of total area of the region is classified as urban, ranging from 0.9 – 1.1%. Figure 8 shows the percentage of total area represented by each LULC change scenario over the greater Lower Mekong region between 1998 and 2018. The LULC can be summarized as 62.1% forest unchanged, 29.1% agricultural area unchanged, 5.8% changed from agriculture to forest, 1.7% changed from forest to agriculture, 0.9% urban unchanged, and the combined land cover change scenarios of urban to forest, urban to agriculture, and agriculture to urban constitute merely 0.3% of the total area.

A logistic regression model was trained and validated for the extents of 18 landslide event inventories. Table 8 presents a summary of the logistic regression coefficients and p-values of all models for the landslide inventory locations with greater than 1000 landslides to avoid potential overfitting from the smaller observation counts. The logistic regression model results for each of the 18 inventories are provided individually in Online Resource 1. In Table 8, the inventory abbreviations are shown next to the corresponding values for the minimum and maximum coefficient and p-value for each category within the factors. From this table, Muong Lat (MT) represents the highest coefficients in the land cover change corresponding to forest (no change), agriculture to forest, and agriculture (no change). When examining the LULC over the inventory location, the landslides largely occur in a forested area with no variation in land cover. The land cover in the Muong Lat (MT) area is fairly homogenous with minimal area represented by the land cover change scenarios other than forest (no change). However, several landslides did occur within areas that underwent deforestation for agriculture and in invariable agricultural areas. The model trained with the Da Bac (DB) inventory produces minimum coefficients for all distance to roads categories which indicates that in this area, the presence of roads is not very influential on landslide occurrence. When examining the Da Bac (DB) location, there is an ample road network throughout the

province, but the landslide distribution does not appear to be influenced by the presence or absence of roads and the landslides do not cluster around roads.

Furthermore, Mu Chang Chai (MC) contributes to the minimum coefficients for the slope categories which could indicate that slope is less influential in this location, even though the p-values corresponding to the slope factor were not significant. The inventory mapped in Mu Chang Chai (MC) occurred in a mountainous forested area with varying slope. The inventory in Mu Chang Chai (MC) produced the highest coefficient for forest loss and the minimum p-value which could be explained by a large cluster of landslides occurring around an area that had experienced substantial forest loss in the years prior to the event. Mu Chang Chai (MC) also represents the maximum coefficients for proximity to roads indicating that roads are more influential on landslides in this location compared to other inventories. When looking closely at the area, the landslide distribution appears to be influenced by proximity to the road network. However, the p-values corresponding to distance to roads in the Mu Chang Chai (MC) inventory indicate this factor was not found to be statistically significant in the logistic regression model. Overall, the coefficients for distance to roads decrease with distance indicating that road proximity has an influence on landslide occurrence. This would agree with the findings of Larsen & Parks (1997) which identified that landslide frequency decreased as distance to roads increased in Puerto Rico.

The Logistic Regression models were validated using 30 % of the landslide inventories as well as randomly generated non-landslide points. The models were validated by plotting the true positive rate versus the false positive rate (ROC) and calculating the area under the resulting curve (AUC). The AUC values from the validation of the Logistic Regression model and the number of landslides within each landslide inventory are presented in Table 9. The model validation results found all AUC values to be estimated above 0.7 except for one inventory in Hakha, Myanmar with an AUC value equal to 0.697. This was the lowest AUC amongst the model results indicating the model trained for Hakha, Myanmar did not perform as well compared to the other locations. The model trained for Thaphabath, Laos outperformed the other models based on having the highest AUC value of 0.958. The average AUC value of all 18 models is 0.82. Based on the model validation results in Table 9, the number of landslides and AUC values are not correlated indicating the number of landslides within each location used to train the models did not affect the model performance.

5.0 Discussion

The land cover of the inventories used in this study were dominated by forests with minimal LULC changes present. According to Table 5, the scenarios of LULC change from forest to urban, agriculture to urban, urban to forest, and urban to agriculture combined make up only 0.082 % of the total area averaged over the 18 inventory locations. Looking at the LULC analysis over the LMRB in Figure 6 and Figure 7, the relatively small area occupied by urban areas may make it difficult to see any conclusive patterns in landslide activity. The LULC scenarios involving urban activities were less prominent in the landslide inventories used in this study, but also occupy the lowest amount of total land area in the greater Lower Mekong region so this category is not only less represented in the 18 landslide inventory area locations, but overall in the Lower Mekong River Basin. The

amount of area occupied by urban and built-up classification is not comparable to the amount of agricultural and forested areas in the LMRB. Additionally, the scenario involving urban activities did not experience any landslides within the 18 inventories used in this study. Therefore, the impact of LULC change scenarios to or from the urban classification cannot be fully determined using the 18 inventories presented in this study.

The Frequency Ratio (FR) reveals potential correlation between landslide locations and causative factors in the area. Overall, the scenario from agriculture to forest had the highest average FR value followed by the scenario of forest with no change (Figure 5). The forested areas that experienced no change had an average FR value of 2.06 when averaged over all 18 study locations, and this is most likely due to the prevalence of forested mountainous regions with steep slopes where most landslides occur in this region. The results of this study indicate that the land cover change scenario from agriculture to forest could have an impact on landslide occurrence and that areas changing from agriculture to forest may be more susceptible to landslides in the years following the land cover change. This could indicate that abandoned agricultural lands left to naturally recover are more susceptible to landslide activity than other land cover change scenarios, which would be similar to the conclusions drawn by Deng et al. (2018) and Persichillo et al. (2017). Further evaluation of land cover change from agriculture to forest with landslide inventories where this LULC change scenario is more prevalent than the inventories used here needs to be executed to further understand the impact of land use changing from agriculture to forest as invariable forests dominate the areas used in this study. Additionally, the FR being a univariate analysis must be taken into consideration. The areas where landslides occurred that were deforested for agricultural purposes could be influenced by additional factors. Other limitations include the spatial resolution and the availability of remotely-sensed datasets for the region. For example, the finest resolution for publicly available DEM data for the Lower Mekong River Basin is 30 meters, which is much coarser than other regions such as USA with one-meter DEM available. With landslides ranging in size, coarser spatial resolutions may not accurately represent the environment of very small, shallow slope failures. Enhanced spatial resolution of remotely sensed data would greatly benefit modelling efforts for landslide susceptibility in the Lower Mekong River Basin.

We can make generalized conclusions for the 18 inventory locations and models regarding landslide causative factors using the coefficients and p-values from Table 8. When averaged over all 18 models the causative factors associated with distance to roads, forest loss, and slope display positive coefficients, which is expected considering these variables are known to be influential on landslide occurrence. Overall, the most significant variables based on the mean p-values were slope and aspect. The high significance of aspect could be explained by the models using flat as the basis factor. When considering all 18 inventories, the logistic regression models did not indicate that areas changing from agriculture to forest were as influential on landslide occurrence as the FR analysis did, which could be explained by the FR being a univariate analysis and the Logistic Regression being multivariate. However, the average coefficient for the LULC change category of agriculture to forest has the only positive coefficient of any of the change scenarios besides forest and agriculture with no change. Forest with no LULC change had the highest and only positive average coefficient relative to the other land cover change scenarios which is most likely due to the majority of landslides in this study occurring in steep forested areas and

the considerable amount of forested area throughout the study locations. Areas that changed from forest to urban have the lowest average coefficient which could be explained by the limited number of landslide points within the area represented by this scenario in the inventories. Alternatively, this could mean that areas being developed are not susceptible to landslides due to other factors such as low slope which could indicate informed land management decisions in the region.

6.0 Conclusions

Land use and land cover (LULC) changes can affect slope stability and geological conditions that may influence the occurrence of landslide activity. This study assessed the influence of LULC changes on landslide susceptibility for 18 locations throughout the Lower Mekong River Basin (LMRB). The majority of landslides occurred in the LULC change scenario with the largest land coverage percentage, which is forested areas that did not experience any change in land cover. However, the LULC change scenario from agriculture to forest had the highest FR values overall. Both the FR analysis and LR models indicated that the LULC change scenario from agricultural land to forest could positively correlate with landslide occurrence. However, for real-time analysis the LULC data available on the SERVIR-Mekong Land Cover Portal would be needed to be updated each year as currently, maps are only available only up to 2018.

There were data limitation issues regarding the representation of land cover changes in the extent of the landslide inventories. Not all land cover change scenarios are represented in these study areas, more locations with landslide inventories that experienced land cover changes are needed to fully analyze the influence of LULC on landslide susceptibility. This method can further be applied to new landslide inventories for other locations in the Lower Mekong River Basin as the data becomes available to discover more consistent correlations between LULC change and landslide susceptibility. Specifically, the relationship between agricultural abandonment and landslide occurrence could be further analyzed to determine how this LULC change influences susceptibility in the Lower Mekong Region. The inclusion of dynamic LULC in landslide susceptibility models could greatly improve hazard assessment and should be investigated as the combination of land use changes over time due to population expansion and disturbances caused by climate change. This analysis is done primarily using remote sensing products, making it transferable to other landslide-prone regions around the world. Additional research efforts could further investigate the role of agricultural abandonment and natural recovery on rainfall-triggered shallow landslides.

7.0 Statements and Declarations

All authors contributed to the study conception and design. Material preparation, data collection and analysis were performed by Chelsea Dandridge. The first draft of the manuscript was written by Chelsea Dandridge and all authors commented on previous versions of the manuscript. All authors read and approved the final manuscript. There are no competing interests related to this work.

References

1. Amatya P, Kirschbaum D, Stanley T, Tanyas H (2021) Landslide mapping using object-based image analysis and open source tools. Eng Geol 282:. https://doi.org/10.1016/j.enggeo.2021.106000
2. Amatya P, Kirschbaum D, Stanley T, Tanyas H (2021) Rainfall-induced landslide inventories for Lower Mekong based on Planet imagery and a semi-automatic mapping method. Geosci Data J
3. Bai SB, Wang J, Lü GN, et al (2010) GIS-based logistic regression for landslide susceptibility mapping of the Zhongxian segment in the Three Gorges area, China. Geomorphology 115:23–31. https://doi.org/10.1016/j.geomorph.2009.09.025
4. Batjes NH, Ribeiro E, Van Oostrum A (2020) Standardised soil profile data to support global mapping and modelling (WoSIS snapshot 2019). Earth Syst Sci Data 12:299–320. https://doi.org/10.5194/essd-12-299-2020
5. Bornaetxea T, Rossi M, Marchesini I, Alvioli M (2018) Effective surveyed area and its role in statistical landslide susceptibility assessments. Nat Hazards Earth Syst Sci Discuss 1–22. https://doi.org/10.5194/nhess-2018-88
6. Bruschi VM, Bonachea J, Remondo J, et al (2013) Land management versus natural factors in land instability: Some examples in northern Spain. Environ Manage 52:398–416. https://doi.org/10.1007/s00267-013-0108-7
7. Camilo DC, Lombardo L, Mai PM, et al (2017) Handling high predictor dimensionality in slope-unit-based landslide susceptibility models through LASSO-penalized Generalized Linear Model. Environ Model Softw 97:145–156. https://doi.org/10.1016/j.envsoft.2017.08.003
8. Chen CY, Huang WL (2013) Land use change and landslide characteristics analysis for community-based disaster mitigation. Environ Monit Assess 185:4125–4139. https://doi.org/10.1007/s10661-012-2855-y
9. Chen L, Guo Z, Yin K, et al (2019) The influence of land use and land cover change on landslide susceptibility: A case study in Zhushan Town, Xuan'en County (Hubei, China). Nat Hazards Earth Syst Sci 19:2207–2228. https://doi.org/10.5194/nhess-19-2207-2019
10. Dai FC, Lee CF, Ngai YY (2002) Landslide risk assessment and management: An overview. Eng Geol 64:65–87. https://doi.org/10.1016/S0013-7952(01)00093-X
11. Das G, Lepcha K (2019) Application of logistic regression (LR) and frequency ratio (FR) models for landslide susceptibility mapping in Relli Khola river basin of Darjeeling Himalaya, India. SN Appl Sci 1:1–22. https://doi.org/10.1007/s42452-019-1499-8
12. Degraff J V., Cannon SH, Gartner JE (2015) The timing of susceptibility to post-fire debris flows in the western United States. Environ Eng Geosci 21:277–292. https://doi.org/10.2113/gseegeosci.21.4.277
13. Deng X, Xu D, Zeng M, Qi Y (2018) Landslides and cropland abandonment in China's mountainous areas: Spatial distribution, empirical analysis and policy implications. Sustain 10:. https://doi.org/10.3390/su10113909
14. Felicísimo ÁM, Cuartero A, Remondo J, Quirós E (2013) Mapping landslide susceptibility with logistic regression, multiple adaptive regression splines, classification and regression trees, and maximum entropy methods: A comparative study. Landslides 10:175–189. https://doi.org/10.1007/s10346-012-0320-1
15. Forbes K, Broadhead J, Bischetti GB, et al (2012) The role of trees and forests in the prevention of landslides and rehabilitation of landslide-affected areas in Asia Second edition In collaboration with. For landslides 12–21
16. Froude MJ, Petley DN (2018) Global fatal landslide occurrence from 2004 to 2016. Nat Hazards Earth Syst Sci 18:2161–2181. https://doi.org/10.5194/nhess-18-2161-2018
17. Gariano SL, Petrucci O, Rianna G, et al (2018) Impacts of past and future land changes on landslides in southern Italy. Reg Environ Chang 18:437–449. https://doi.org/10.1007/s10113-017-1210-9

18. Glade T (2003) Landslide occurrence as a response to land use change: A review of evidence from New Zealand. Catena 51:297–314. https://doi.org/10.1016/S0341-8162(02)00170-4

19. Gorsevski P V., Gessler PE, Foltz RB, Elliot WJ (2006) Spatial prediction of landslide hazard using logistic regression and ROC analysis. Trans GIS 10:395–415. https://doi.org/10.1111/j.1467-9671.2006.01004.x

20. Hansen MC, Potapov P V., Moore R, et al (2013) High-resolution global maps of 21st-century forest cover change. Science (80-) 342:850–853. https://doi.org/10.1126/science.1244693

21. Hemasinghe H, Rangali RSS, Deshapriya NL, Samarakoon L (2018) Landslide susceptibility mapping using logistic regression model (a case study in Badulla District, Sri Lanka). Procedia Eng 212:1046–1053. https://doi.org/10.1016/j.proeng.2018.01.135

22. Hengl T, De Jesus JM, Heuvelink GBM, et al (2017) SoilGrids250m: Global gridded soil information based on machine learning

23. Hewawasam T (2010) Effect of land use in the upper Mahaweli catchment area on erosion landslides and siltation in hydropower reservoirs of Sri Lanka. J Natl Sci Found Sri Lanka 38:3–14. https://doi.org/10.4038/jnsfsr.v38i1.1721

24. Highland L, Bobrowsky P (2008) The Landslide Handbook-A Guide to Understanding Landslides. Landslide Handb - A Guid to Underst Landslides 4–42

25. Horafas D, Gkeki T (2017) Applying Logistic Regression for Landslide Susceptibility Mapping . The Case Study of Krathis Watershed , North Peloponnese , Greece. 6:23–28. https://doi.org/10.5923/s.ajgis.201701.03

26. Indhanu T, Chub-Uppakarn T, Chalermyanont T (2020) Geotechnical Analysis of a Landslide in Nakorn Si Thammarat Province, Southern Thailand. Lect Notes Civ Eng 62:923–927. https://doi.org/10.1007/978-981-15-2184-3_120

27. Jaboyedoff M, Michoud C, Derron MH, et al (2016) Human-Induced Landslides: Toward the analysis of anthropogenic changes of the slope environment. Landslides Eng Slopes Exp Theory Pract 1:217–232. https://doi.org/10.1201/b21520-20

28. Karsli F, Atasoy M, Yalcin A, et al (2009) Effects of land-use changes on landslides in a landslide-prone area (Ardesen, Rize, NE Turkey). Environ Monit Assess 156:241–255. https://doi.org/10.1007/s10661-008-0481-5

29. Kean JW, Staley DM, Cannon SH (2011) In situ measurements of post-fire debris flows in southern California: Comparisons of the timing and magnitude of 24 debris-flow events with rainfall and soil moisture conditions. J Geophys Res Earth Surf 116:1–21. https://doi.org/10.1029/2011JF002005

30. Khan H, Shafique M, Khan MA, et al (2019) Landslide susceptibility assessment using Frequency Ratio, a case study of northern Pakistan. Egypt J Remote Sens Sp Sci 22:11–24. https://doi.org/10.1016/j.ejrs.2018.03.004

31. Larsen MC, Parks JE (1997) How wide is a road? The association of roads and mass-wasting in a forested montane environment. Earth Surf Process Landforms 22:835–848. https://doi.org/10.1002/(SICI)1096-9837(199709)22:9<835::AID-ESP782>3.0.CO;2-C

32. Lee S, Sambath T (2006) Landslide susceptibility mapping in the Damrei Romel area, Cambodia using frequency ratio and logistic regression models. Environ Geol 50:847–855. https://doi.org/10.1007/s00254-006-0256-7

33. Lombardo L, Mai PM (2018) Presenting logistic regression-based landslide susceptibility results. Eng Geol 244:14–24. https://doi.org/10.1016/j.enggeo.2018.07.019

34. McAdoo BG, Quak M, Gnyawali KR, et al (2018) Roads and landslides in Nepal: How development affects environmental risk. Nat Hazards Earth Syst Sci 18:3203–3210. https://doi.org/10.5194/nhess-18-3203-2018

35. Meijer JR, Huijbregts MAJ, Schotten KCGJ, Schipper AM (2018) Global patterns of current and future road infrastructure. Environ Res Lett 13:. https://doi.org/10.1088/1748-9326/aabd42

36. Mugagga F, Kakembo V, Buyinza M (2012) Land use changes on the slopes of Mount Elgon and the implications for the occurrence of landslides. Catena 90:39–46. https://doi.org/10.1016/j.catena.2011.11.004

37. NASA JPL (2020) NASADEM Merged DEM Global 1 arc second V001. NASA EOSDIS Land Processes DAAC. Accessed from https://doi.org/10.5067/MEaSUREs/NASADEM/NASADEM_HGT.001

38. Penna D, Borga M, Aronica GT, et al (2014) The influence of grid resolution on the prediction of natural and road-related shallow landslides. Hydrol Earth Syst Sci 18:2127–2139. https://doi.org/10.5194/hess-18-2127-2014

39. Persichillo MG, Bordoni M, Meisina C (2017) The role of land use changes in the distribution of shallow landslides. Sci Total Environ 574:924–937. https://doi.org/10.1016/j.scitotenv.2016.09.125

40. Pisano L, Zumpano V, Malek, et al (2017) Variations in the susceptibility to landslides, as a consequence of land cover changes: A look to the past, and another towards the future. Sci Total Environ 601–602:1147–1159. https://doi.org/10.1016/j.scitotenv.2017.05.231

41. Pourghasemi HR, Moradi HR, Fatemi Aghda SM (2013) Landslide susceptibility mapping by binary logistic regression, analytical hierarchy process, and statistical index models and assessment of their performances. Nat Hazards 69:749–779. https://doi.org/10.1007/s11069-013-0728-5

42. Prastica RMS, Apriatresnayanto R, Marthanty DR (2019) Structural and green infrastructure mitigation alternatives prevent Ciliwung River from water-related landslide. Int J Adv Sci Eng Inf Technol 9:1825–1832. https://doi.org/10.18517/ijaseit.9.6.8413

43. Reichenbach P, Busca C, Mondini AC, Rossi M (2014) The Influence of Land Use Change on Landslide Susceptibility Zonation: The Briga Catchment Test Site (Messina, Italy). Environ Manage 54:1372–1384. https://doi.org/10.1007/s00267-014-0357-0

44. Reichenbach P, Rossi M, Malamud BD, et al (2018) A review of statistically-based landslide susceptibility models. Earth-Science Rev 180:60–91. https://doi.org/10.1016/j.earscirev.2018.03.001

45. Saah D, Tenneson K, Poortinga A, et al (2020) Primitives as building blocks for constructing land cover maps. Int J Appl Earth Obs Geoinf 85:101979. https://doi.org/10.1016/j.jag.2019.101979

46. Shahabi H, Khezri S, Ahmad B Bin, Hashim M (2014) Landslide susceptibility mapping at central Zab basin, Iran: A comparison between analytical hierarchy process, frequency ratio and logistic regression models. Catena 115:55–70. https://doi.org/10.1016/j.catena.2013.11.014

47. Shu H, Hürlimann M, Molowny-Horas R, et al (2019) Relation between land cover and landslide susceptibility in Val d'Aran, Pyrenees (Spain): Historical aspects, present situation and forward prediction. Sci Total Environ 693:1–14. https://doi.org/10.1016/j.scitotenv.2019.07.363

48. Silalahi FES, Pamela, Arifianti Y, Hidayat F (2019) Landslide susceptibility assessment using frequency ratio model in Bogor, West Java, Indonesia. Geosci Lett 6:. https://doi.org/10.1186/s40562-019-0140-4

49. Spruce J, Bolten J, Mohammed IN, et al (2020) Mapping Land Use Land Cover Change in the Lower Mekong Basin From 1997 to 2010. Front Environ Sci 8:. https://doi.org/10.3389/fenvs.2020.00021

50. Spruce J, Bolten J, Srinivasan R, Lakshmi V (2018) Developing land use land cover maps for the lower mekong basin to aid hydrologic modeling and basin planning. Remote Sens 10:. https://doi.org/10.3390/rs10121910

51. Winter MG, Dixon N, Wasowski J, Dijkstra TA (2010) Introduction to land-use and climate change impacts on landslides. Q J Eng Geol Hydrogeol 43:367–370. https://doi.org/10.1144/1470-9236/10-035

52. Yan L, Xu W, Wang H, et al (2019) Drainage controls on the Donglingxing landslide (China) induced by rainfall and fluctuation in reservoir water levels. Landslides 16:1583–1593

53. Zhou C, Yin K, Cao Y, et al (2018) Landslide susceptibility modeling applying machine learning methods: A case study from Longju in the Three Gorges Reservoir area, China. Comput Geosci 112:23–37. https://doi.org/10.1016/j.cageo.2017.11.019

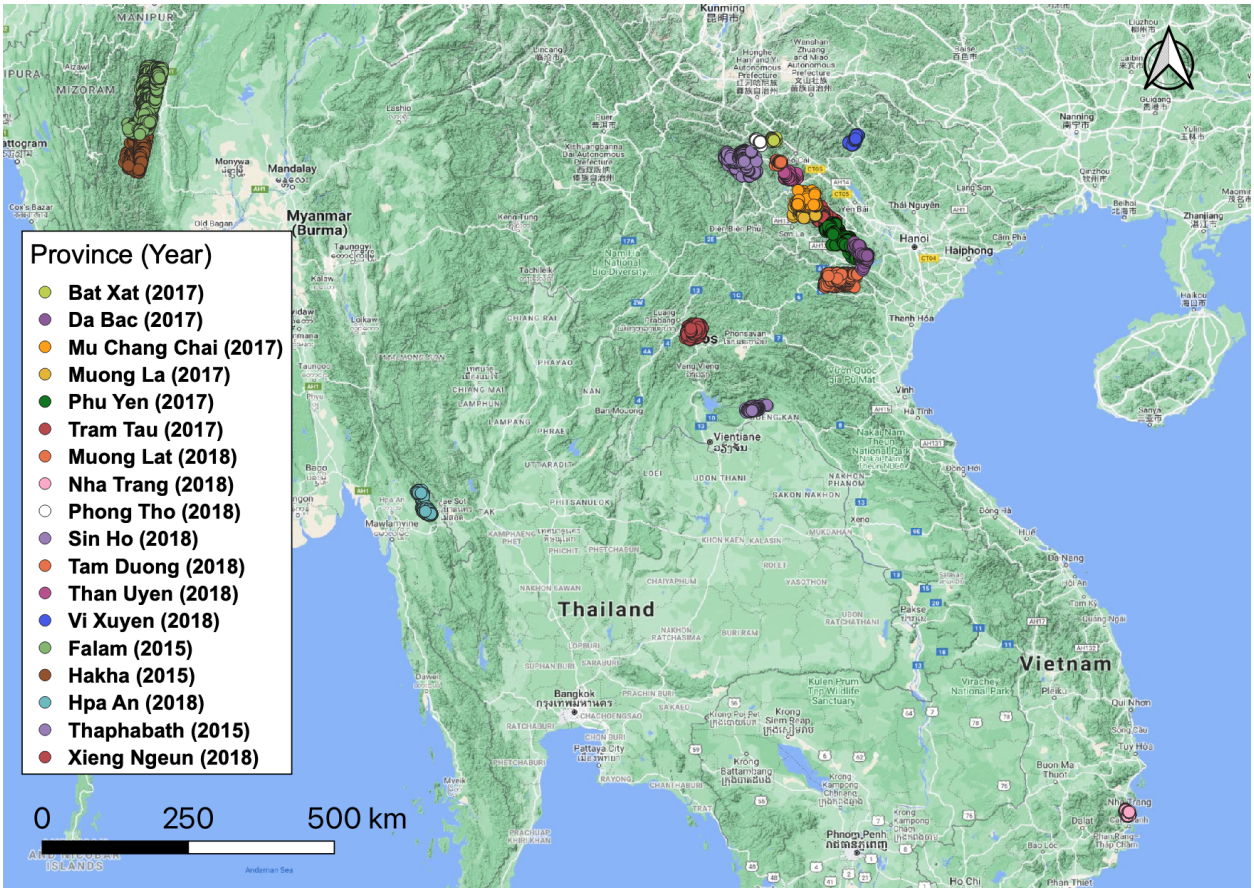

Figure I. Geographic locations of the landslide inventories in the LMRB

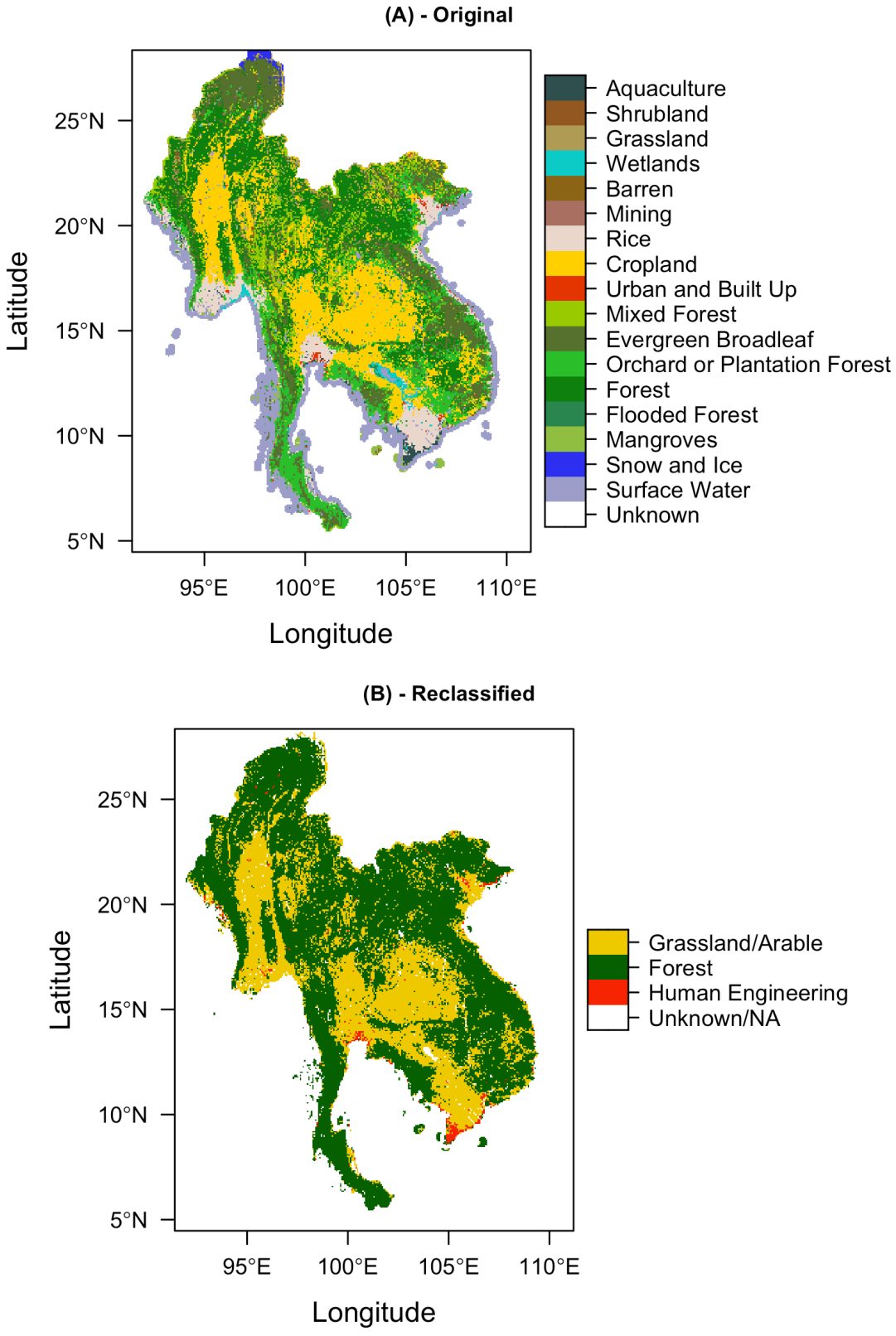

Figure II. (A) The original LULC classifications and (B) the reclassified LULC classifications for the LMRB region in 2018.

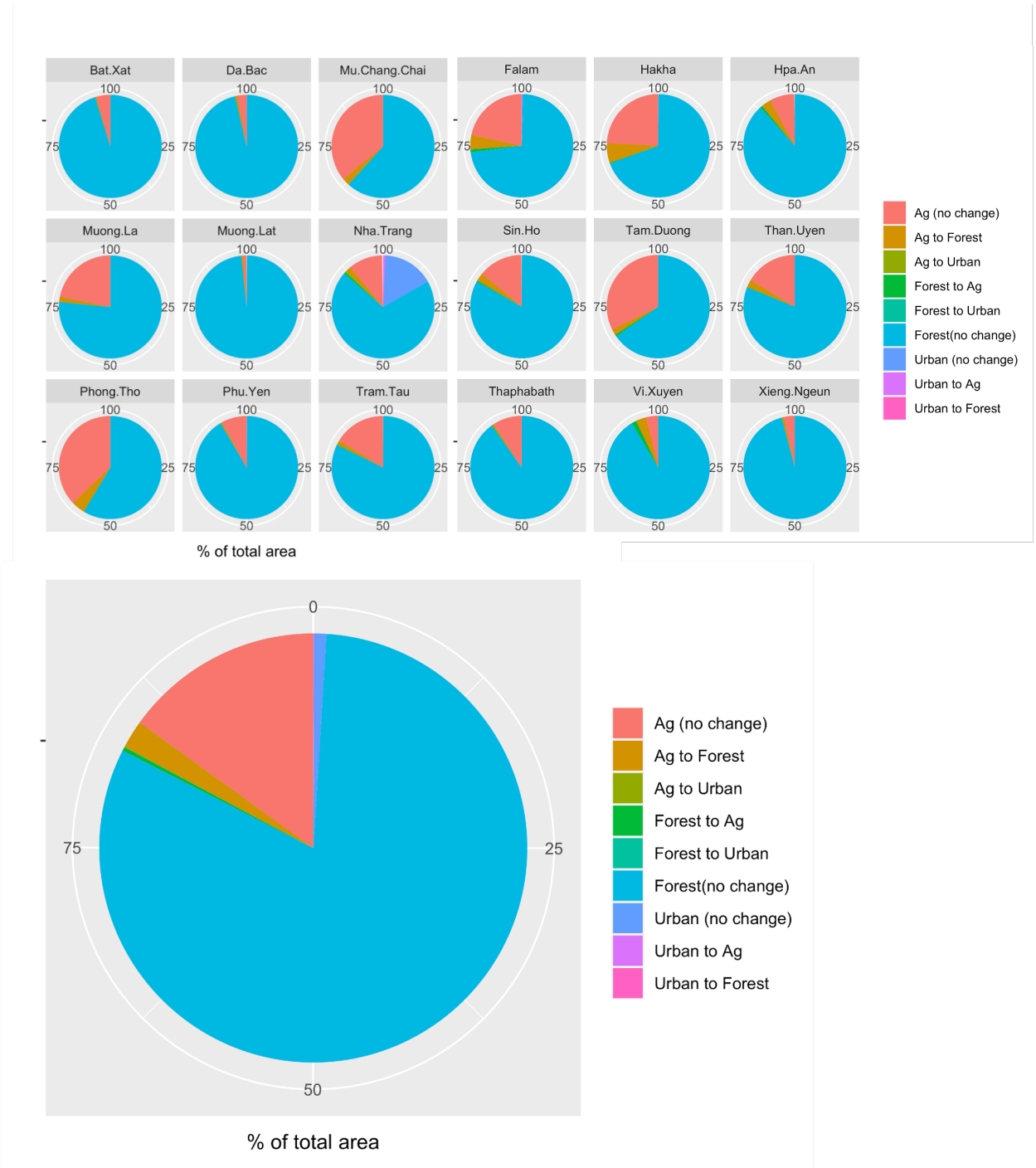

Figure III. (A) Percentage of area for each LULC change scenario over 10 years for each inventory location (B) Percentage of area of each LULC change scenario averaged over all locations.

Table I. Landslide inventory description				
District	**Country**	**Year**	**Satellite**	**Landslides**
(BX) Bat Xat	Vietnam	2017	PlanetScope	99
(DB) Da Bac	Vietnam	2017	RapidEye	1086
(MC) Mu Chang Chai	Vietnam	2017	RapidEye	1256
(ML) Muong La	Vietnam	2017	RapidEye	758
(PY) Phu Yen	Vietnam	2017	RapidEye	1368
(TT) Tram Tau	Vietnam	2017	RapidEye	1490
(MT) Muong Lat	Vietnam	2018	PlanetScope	1718
(NT) Nha Trang	Vietnam	2018	PlanetScope	207
(PT) Phong Tho	Vietnam	2018	PlanetScope	302
(SH) Sin Ho	Vietnam	2018	RapidEye	707
(TD) Tam Duong	Vietnam	2018	PlanetScope	159
(TU) Than Uyen	Vietnam	2018	PlanetScope	312
(VX) Vi Xuyen	Vietnam	2018	PlanetScope	157
(FM) Falam	Myanmar	2015	RapidEye	5086
(HK) Hakha	Myanmar	2015	RapidEye	1737
(HA) Hpa-An	Myanmar	2018	PlanetScope	992
(TB) Thaphabath	Laos	2015	RapidEye	242
(XN) Xieng Ngeun	Laos	2018	PlanetScope	1178

Table II. Data descriptions, resolutions, and sources			
Dataset	**Derived variables**	**Spatial resolution**	**Source**
DEM [raster]	Slope Aspect	30 m	NASA JPL (2020)
Land cover [raster]	Land use/land cover change (LULC)	30 m	Saah et al. (2020)
Roads [vector]	Distance to roads	--	Meijer (2018)
Soil properties [raster]	Bulk density Organic carbon	250 m	Hengl (2017)
Forest Cover [raster]	Forest cover loss	30 m	Hansen et al. (2013)

Table III. Reclassification of land cover categories	
New classification	**Original classification**
Urban	Urban and built up Mining Aquaculture
Agriculture	Cropland Grassland Shrubland
Forest	Forest Evergreen Broadleaf Mixed Forest Orchard or Plantation Forest

Table IV. Classification of factors for model input variables				
Distance To Roads	**Forest Cover**	**Slope**	**Aspect**	**Land Cover Change**
< 10 m	no loss (0)	0° - 10°	flat (-1)	Urban (no change)
10 - 50 m	loss (1)	20° - 25°	north (0 - 22.5)	Urban to Forest
50 - 100 m		25° - 40°	northeast (22.5 - 67.5)	Urban to Agriculture
100 - 200 m		40° - 65°	east (67.5-112.5)	Forest to Urban
200 - 1000 m		> 65°	southeast (112.5 - 157.5)	Forest (no change)
> 1000 m			south (157.5 - 202.5)	Forest to Agriculture
			southwest (202.5 - 247.5)	Agriculture to Urban
			west (247.5 - 292.5)	Agriculture to Forest
			northwest (292.5 - 337.5)	Agriculture (no change)
			north (337.5 - 360)	

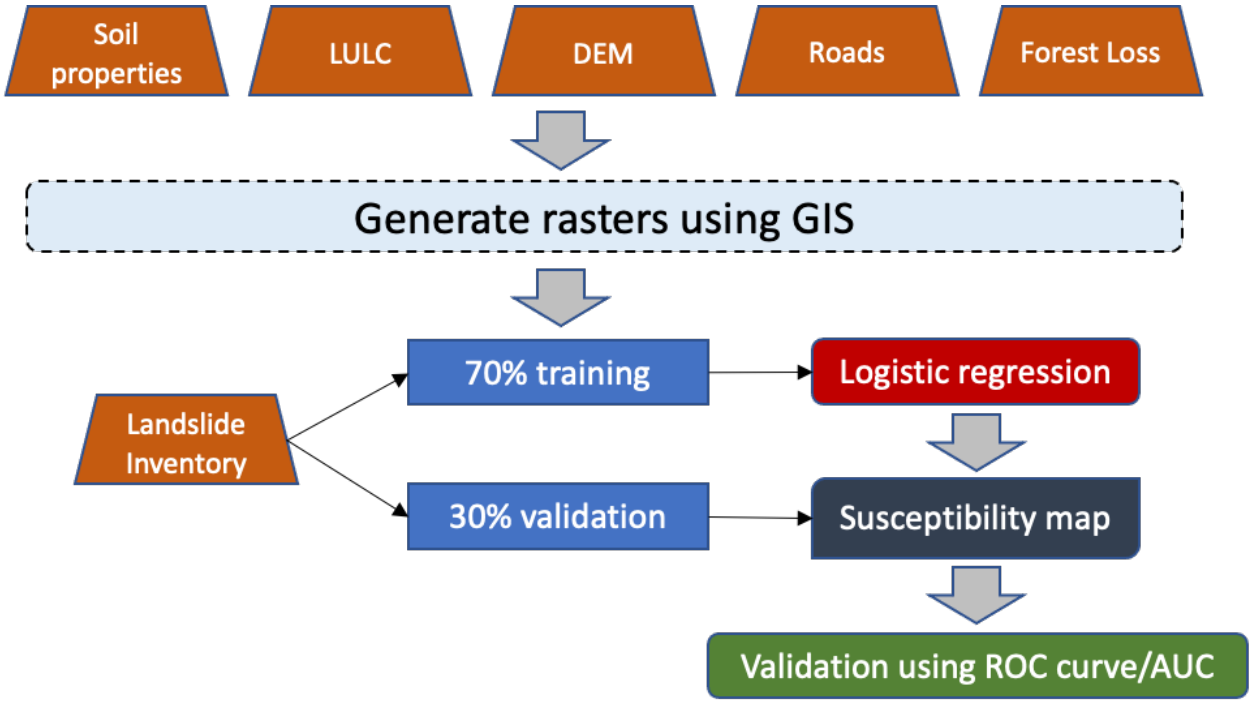

Figure IV. Workflow diagram for logistic regression modelling of landslide susceptibility

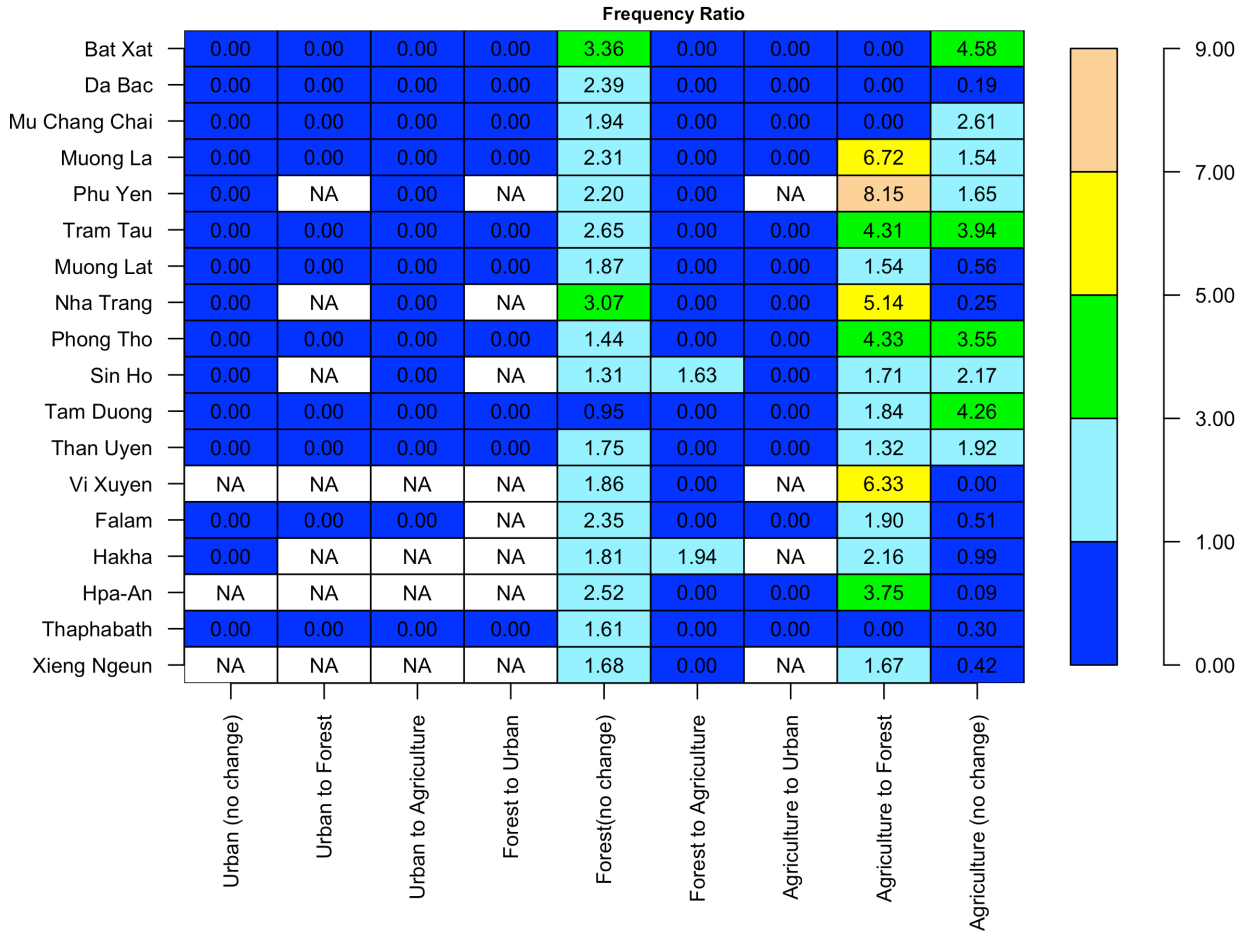

Figure V. Matrix diagram displaying the FR for each landslide inventory location and LULC change scenario. FR values < 1 are represented by dark blue and no data values by 'NA' in white.

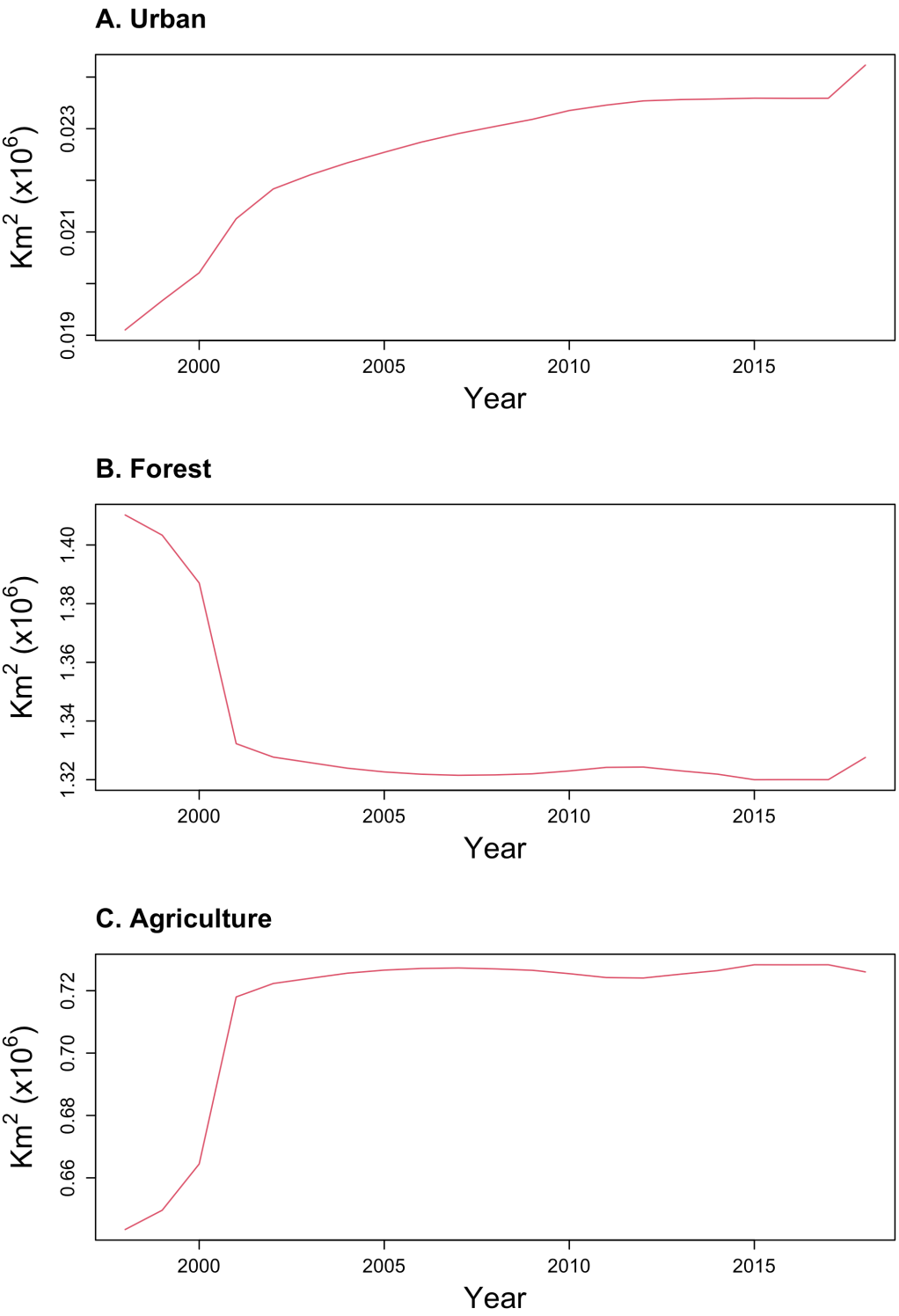

Figure VI. (A) Total area of Lower Mekong Region with classification of Urban (km^2), (B) Total area of Lower Mekong Region with classification of Forest (km^2), and (C) Total area of Lower Mekong Region with classification of Agriculture (km^2) time series from 1998 to 2018, scaled to observe patterns within each classification.

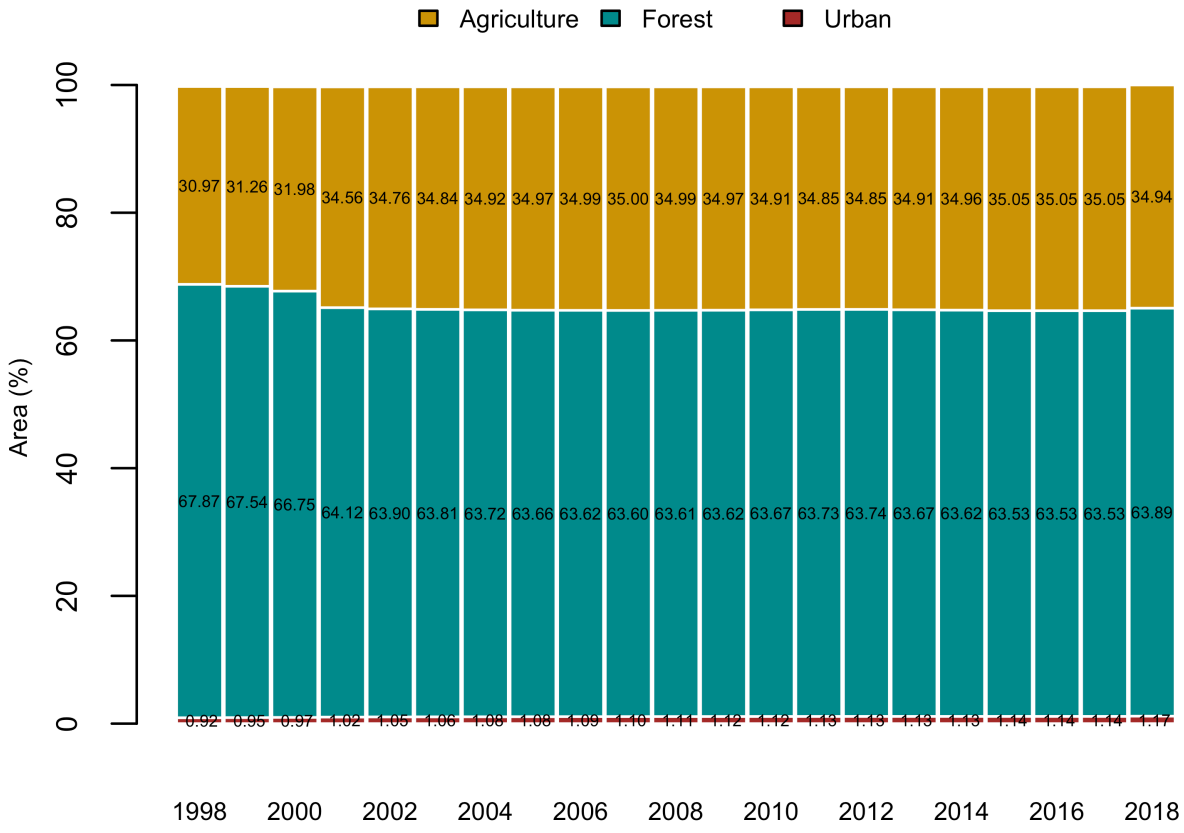

Figure VII. Bar plot of the percentage of total area of each land cover classification within the Lower Mekong River Basin annually from 1998 to 2018.

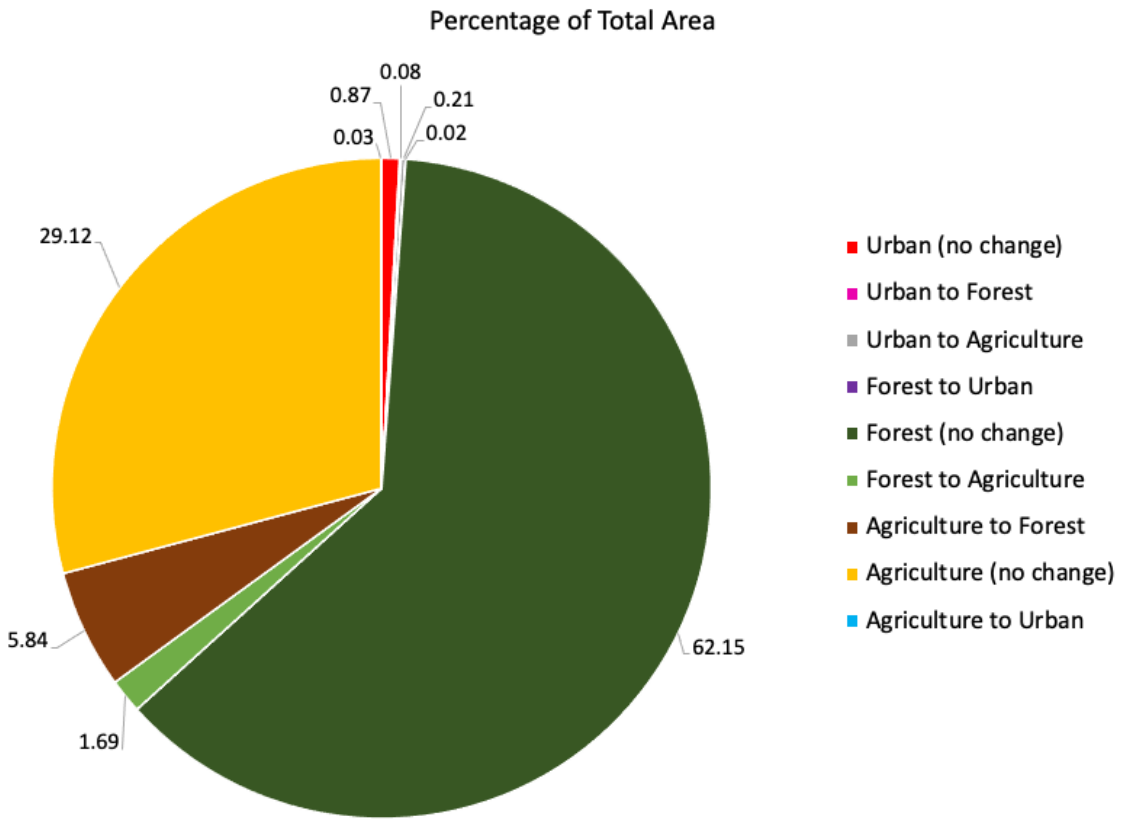

Figure VIII. Pie chart depicting the percentage of total area represented by each LULC change scenario over the greater Lower Mekong region between 1998 and 2018.

Table V. Mean percentage of total area averaged over all locations			
LULC change scenario over 10 years			
	Urban	Forest	Agriculture
Urban	0.93 %	0.003 %	0.05 %
Forest	0 %	81.48 %	0.31 %
Agriculture	0.03 %	2.11 %	15.05 %

Table VI. Sum of landslides within all locations			
LULC change scenario over 10 years			
	Urban	Forest	Agriculture
Urban	0	0	0
Forest	0	15,568	6
Agriculture	0	614	2,530

Table VII. Mean Frequency Ratio averaged over all locations			
LULC change scenario over 10 years			
	Urban	Forest	Agriculture
Urban	NA	NA	NA
Forest	NA	2.06	0.20
Agriculture	NA	2.83	1.64

Table VIII. Summary of Logistic Regression Coefficients and P-Values over all inventory locations							
Factor	Category	Coefficient			P-value		
		min	max	mean	min	max	mean
Intercept	Intercept	-21.78 MT	-2.84 DB	-13.02	1.99E-05 PY	9.83E-01 MC	6.24E-01
Land Cover Change	Urban to Forest	-9.76 FM	0.71 MT	-3.51	8.02E-02 PY	1.00E+00 MT	6.88E-01
	Forest to Urban	-15.73 PY	-9.11 FM	-12.63	9.73E-01 PY	9.84E-01 HK	9.79E-01
	Forest (no change)	-0.61 DB	16.33 MT	5.48	6.71E-06 FM	9.87E-01 MT	4.29E-01
	Forest to Agriculture	-13.65 XN	3.99 MT	-5.41	4.39E-01 FM	9.98E-01 TT	8.83E-01
	Agriculture to Urban	-13.12 PY	-10.58 FM	-12.02	9.71E-01 FM	9.91E-01 PY	9.82E-01
	Agriculture to Forest	-15.46 MC	16.01 MT	0.26	3.39E-05 FM	9.87E-01 MT	5.03E-01
	Agriculture (no change)	-1.29 DB	14.79 MT	3.76	2.20E-25 MC	9.88E-01 MT	3.19E-01
Distance to Road	20 - 50 m	-2.06 DB	15.54 MC	4.15	5.20E-02 DB	9.86E-01 MC	6.50E-01
	50 - 100 m	-1.04 DB	15.65 MC	2.73	1.67E-01 FM	9.86E-01 MC	6.05E-01
	100 - 200 m	-1.30 DB	16.02 MC	4.21	1.77E-01 DB	9.86E-01 MT	6.76E-01
	200 - 1000 m	-0.65 DB	16.30 MC	4.53	3.80E-01 FM	9.85E-01 MC	6.79E-01
	> 1000 m	-1.19 DB	15.86 MC	5.45	2.20E-01 DB	9.87E-01 XN	6.39E-01
Soil Bulk Density	60 - 100 cg/cm^3	-1.13 PY	-0.88 FM	-1.01	1.12E-01 PY	3.61E-01 FM	2.36E-01
	100-130 cg/cm^3	-1.32 FM	1.28 MT	-0.36	2.28E-18 MC	6.77E-01 DB	2.93E-01
Forest Loss	forest loss = 1	-0.77 FM	2.48 MC	0.67	4.13E-14 MC	4.73E-01 HK	6.47E-02
Slope	10 - 20 deg	0.58 DB	2.07 XN	1.41	1.26E-15 FM	1.95E-01 DB	2.76E-02
	20-25 deg	0.49 MC	3.17 MT	2.12	2.95E-24 FM	7.29E-02 MC	9.13E-03
	25 - 40 deg	0.22 MC	4.09 MT	2.70	5.15E-32 FM	3.93E-01 MC	4.92E-02
	40 - 65 deg	0.40 MC	4.42 DB	2.97	2.30E-27 FM	3.67E-01 MC	4.59E-02
	> 65 deg	-15.52 MC	3.33 XN	-9.60	2.41E-02 XN	9.93E-01 PY	8.33E-01
Aspect	North	-2.20 TT	-0.64 FM	-1.24	9.32E-06 FM	1.34E-01 XN	3.20E-02
	East	0.35 HK	1.85 DB	1.16	1.69E-12 FM	3.09E-02 HK	3.87E-03
	Southeast	0.96 HK	2.90 DB	1.94	3.18E-26 FM	1.34E-09 HK	1.68E-10
	South	0.53 HK	3.12 DB	1.80	5.27E-21 DB	1.32E-03 HK	1.66E-04
	Southwest	-0.12 HK	2.48 DB	1.27	4.77E-14 XN	5.11E-01 HK	6.39E-02
	West	-0.53 HK	1.64 XN	0.24	1.70E-08 XN	4.43E-01 PY	1.51E-01
	Northwest	-2.50 TT	0.98 XN	-0.86	1.77E-06 HK	5.95E-01 MC	7.78E-02

*Color coded abbreviations correspond to the landslide inventories in Table 9
**Red mean values represent the maximum within each factor and blue mean values represent the minimum within each factor

Table IX. Model validation results (AUC) for each inventory location			
District	**Country**	**Landslides**	**AUC**
(BX) Bat Xat	Vietnam	99	0.820
(DB) Da Bac	Vietnam	1086	0.892
(MC) Mu Chang Chai	Vietnam	1256	0.854
(ML) Muong La	Vietnam	758	0.835
(PY) Phu Yen	Vietnam	1368	0.856
(TT) Tram Tau	Vietnam	1490	0.844
(MT) Muong Lat	Vietnam	1718	0.794
(NT) Nha Trang	Vietnam	207	0.853
(PT) Phong Tho	Vietnam	302	0.906
(SH) Sin Ho	Vietnam	707	0.816
(TD) Tam Duong	Vietnam	159	0.838
(TU) Than Uyen	Vietnam	312	0.713
(VX) Vi Xuyen	Vietnam	157	0.755
(FM) Falam	Myanmar	5086	0.732
(HK) Hakha	Myanmar	1737	0.697
(HA) Hpa-An	Myanmar	992	0.869
(TB) Thaphabath	Laos	242	0.958
(XN) Xieng Ngeun	Laos	1178	0.740

* Colors correspond to landslide inventories highlighted in Table 8